Phosphatidylcholine Acyl Unsaturation Modulates the Decrease in Interfacial Elasticity Induced by Cholesterol

Janice M. Smaby, Maureen M. Momsen, Howard L. Brockman, and Rhoderick E. Brown

The Hormel Institute, University of Minnesota, Austin, Minnesota 55912 USA

ABSTRACT The effect of cholesterol on the interfacial elastic packing interactions of various molecular species of phosphatidylcholines (PCs) has been investigated by using a Langmuir-type film balance and analyzing the elastic area compressibility moduli (C_s^{-1}) as a function of average cross-sectional molecular area. Emphasis was on the high surface pressure regions ($\pi \geq 30$ mN/m) which are thought to mimic biomembrane conditions. Increasing levels of cholesterol generally caused the in-plane elasticity of the mixed monolayers to decrease. Yet, the magnitude of the cholesterol-induced changes was markedly dependent upon PC hydrocarbon structure. Among PC species with a saturated sn-1 chain but different sn-2 chain cis unsaturation levels [e.g., myristate (14:0), oleate (18:1$^{\Delta 9(c)}$), linoleate (18:2$^{\Delta 9,12(c)}$), arachidonate (20:4$^{\Delta 5,8,11,14(c)}$), or docosahexenoate (22:6$^{\Delta 4,7,10,13,16,19(c)}$)], the in-plane elasticity moduli of PC species with higher sn-2 unsaturation levels were less affected by high cholesterol mol fractions (e.g., >30 mol %) than were the more saturated PC species. The largest cholesterol-induced decreases in the in-plane elasticity were observed when both chains of PC were saturated (e.g., di-14:0 PC). When both acyl chains were identically unsaturated, the resulting PCs were 20–25% more elastic in the presence of cholesterol than when their sn-1 chains were long and saturated (e.g., palmitate). The mixing of cholesterol with PC was found to diminish the in-plane elasticity of the films beyond what was predicted from the additive behavior of the individual lipid components apportioned by mole and area fraction. Deviations from additivity were greatest for di-14:0 PC and were least for diarachidonoyl PC and didocosahexenoyl PC. In contrast to C_s^{-1} analyses, sterol-induced area condensations were relatively unresponsive to subtle structural differences in the PCs at high surface pressures. C_s^{-1} versus average area plots also indicated the presence of cholesterol concentration-dependent, low-pressure (<14 mN/m) phase boundaries that became more prominent as PC acyl chain unsaturation increased. Hence, area condensations measured at low surface pressures often do not accurately portray which lipid structural features are important in the lipid-sterol interactions that occur at high membrane-like surface pressures.

INTRODUCTION

When faced with external temperatures that deviate from normal physiological conditions, mammalian cells adjust the lipid composition of their membranes to maintain functional integrity. The two most common means by which cells alter their membrane lipid composition are by modifying phosphoglyceride molecular structure and/or by adjusting sterol content. Hence, defining the nature of the changes that cholesterol brings to lipid membranes has been the focus of intense investigation for many years. Indeed, one of the first membrane biophysical effects attributed to cholesterol was its ability to condense the average cross-sectional area of fluid-phase phosphatidylcholines (PCs) (e.g., for review, see Phillips, 1972). Such findings were deduced from Langmuir film balance studies in which the

average, cross-sectional molecular areas of films comprised of cholesterol and phosphoglyceride were shown to decrease below what was predicted by summing the known molecular areas of the pure lipid components (apportioned by mol fraction in the mixture). Subsequently, the monolayer area condensation approach was used to investigate how alterations in phosphoglyceride acyl structure affect interaction with cholesterol (e.g., Chapman et al., 1969; Demel et al., 1972; Ghosh et al., 1973; Evans et al., 1987).

In our recent studies of sterol-sphingomyelin and sterol-phosphatidylcholine mixtures (Smaby et al., 1994), we noted that, when the sn-1 chain of PC was long and saturated, varying the cis unsaturation level of the sn-2 chain had relatively little impact on the resulting apparent area condensation induced by cholesterol. At equimolar cholesterol, only slight differences were observed in the apparent molecular area condensations of dimyristoyl PC (di14:0 PC), 1-myristoyl-2-palmitoyl PC (14:0–16:0 PC), dipalmitoyl PC (di16:0 PC), 1-palmitoyl-2-oleoyl PC (16:0–18:1 PC), and 1-palmitoyl-2-arachidonoyl PC (16:0–20:4 PC) at surface pressures where the PCs themselves were liquid-expanded. We also observed similar results in the cholesterol-induced, apparent area condensations of sphingomyelins (SMs) and galactosylceramides (GalCers) with acyl chains containing zero, one, or two cis double bonds (Smaby et al., 1996b). The findings suggest that, at surface pressures mimicking those occurring in biomembranes

(e.g., $\pi > 30$ mN/m), cholesterol interacts with PCs and simple sphingolipids in a manner that renders area condensation measurements relatively insensitive to structural changes introduced into the sn-2 acyl chain of PC and the N-acyl chains of simple sphingolipids. Because these findings suggest a possible in-plane, dynamic orientation when cholesterol encounters PCs in which one acyl chain is saturated, we have extended this earlier work by studying the "condensing effect" of cholesterol on a variety of fluid-phase PCs containing acyl chains that are sn-1 saturated-sn-2 unsaturated, di-saturated, or di-unsaturated.

Aside from relying solely on cholesterol-induced area condensation measurements, we also have investigated the interfacial elasticity of the various PC species in the presence of increasing cholesterol mol fractions to assess how acyl structure and configuration of phosphoglycerides affect interactions with sterol. From earlier work involving a few select PC molecular species, it is clear the mechano-elastic properties of lipid assemblies, such as the lateral compressibility or its inverse function, the area dilation, reflect the structural features and interactions of their component lipids in very sensitive ways (Kwok and Evans, 1981; Evans and Needham, 1987). The micropipette aspiration technique has provided valuable insights, not only into the bending and shear forces that bilayers can withstand, but also into the in-plane elastic packing interactions within PC bilayers as well as the changes brought about by altering acyl chain composition or cholesterol content (e.g., Evans and Needham, 1987; Needham, 1995, and references within). Recently, we pointed out certain advantages of studying lipid elastic packing interactions by the monolayer approach and demonstrated its utility by evaluating the behavior of various pure GalCers and SMs, as well as select PCs containing saturated or monounsaturated acyl chains (Smaby et al., 1996a). Here, we show how this quantitative approach can be used to gain new insights into the in-plane interactions that occur between cholesterol and PCs containing acyl chains of various structure. In doing so, we show how measurements of interfacial elasticity provide results that differ from monolayer area condensation data yet complement and expand upon the insights provided by the micropipette aspiration studies in systems where formation of stable unilamellar bilayer vesicles may be difficult or impossible. The data also are discussed within the context of other bilayer (Keough et al., 1989; Mitchell et al., 1992; Litman and Mitchell, 1996) and molecular dynamics studies (Robinson et al., 1995) involving sterol/PC interactions.

MATERIALS AND METHODS

All phosphatidylcholines were purchased from Avanti Polar Lipids (Alabaster, AL). Cholesterol was obtained from NuChek Prep (Elysian, MN). Lipid purity was greater than 99% based on thin-layer chromatography. The acyl compositions were analyzed by quantitatively releasing, methylating, and analyzing the fatty acyl residues via capillary gas chromatography as described by Smaby et al. (1996a). Quantitation of cholesterol was by dry weight and of PCs was by phosphate analysis (Bartlett, 1959).

Langmuir film balance conditions

PC and cholesterol stock solutions were prepared in ethanol/hexane (5:95) (Burdick Jackson Laboratories, Muskegon, MI). The ethanol was distilled from zinc and KOH. Solvent purity was verified by dipole potential measurements (Smaby and Brockman, 1991a). Water for the subphase buffer was purified by reverse osmosis, activated charcoal adsorption, and mixed-bed deionization, then passed through a Milli-Q UV Plus System (Millipore Corp., Bedford, MA), and filtered through a 0.22-μm Millipak 40 Membrane. Subphase buffer (pH 6.6) consisting of 10 mM potassium phosphate, 100 mM NaCl, and 0.2% NaN$_3$ was stored under argon until use.

Surface pressure-molecular area-surface potential (π-A) isotherms were measured under a humidified argon atmosphere using a computer-controlled, Langmuir-type film balance, calibrated according to the equilibrium spreading pressures of known lipid standards (Smaby and Brockman, 1990) and housed in a laboratory with a filtered air supply. Lipids were spread in 51.67-μl aliquots of hexane/ethanol (95:5). Films were compressed at a rate of ≤ 4 Å^2/molecule/min after an initial delay period of 4 min. The subphase was maintained at 24 $\pm$ 1°C using a thermostatted, circulating water bath. Dipole potentials were measured using a ^{210}Po ionizing electrode.

Analysis of isotherms

To assess the cross-sectional area condensations induced by cholesterol, mixed lipid monolayers were analyzed by classical average molecular area versus composition diagrams (e.g., Phillips, 1972). Experimentally observed areas of the mixtures were compared with areas calculated by summing the molecular areas of the pure components (apportioned by mol fraction in the mix). The calculated, average molecular area (A) of two-component mixtures was determined at a given surface pressure (π) using the following equation:

$$\text{calc. av.}\quad A = X_1(A_1)_\pi + (1 - X_1)(A_2)_\pi \qquad (1)$$

where X_1 is the mol fraction of component 1 and $(A_1)_\pi$ and $(A_2)_\pi$ are the molecular areas of pure components 1 and 2 at identical surface pressures. Negative deviations from additivity indicated area condensation and implied intermolecular accommodation and/or dehydration interactions between lipids in the mixed films (e.g., Cadenhead and Müller-Landau, 1980).

The apparent cholesterol-induced condensations of the various PC species were calculated at the indicated surface pressure as reported by Phillips and co-workers (Lund-Katz et al., 1988):

PC Area Condensation

$$= A_{PC} - [(A_{mix} - (A_{chol}X_{chol}))/X_{PC}] \qquad (2)$$

where PC condensation units are Å^2/PC molecule, A_{PC} is the area/molecule of the pure PC species, A_{mix} is the average area/molecule of the PC/Chol mixed monolayer, A_{chol} is the area/molecule of the pure cholesterol, X_{chol} is the mol fraction of cholesterol in the mixed monolayer, and X_{PC} is the mol fraction of phospholipid in the mixed film. The net result is to express and normalize cholesterol-induced area condensation as area change imparted to the PC molecule (Lund-Katz et al., 1988; Evans et al., 1987). Although the approach may oversimplify the partial area contribution of cholesterol, π-A measurements of pure cholesterol do show very similar average molecular areas at both low and high pressures (Pethica, 1955; Phillips, 1972). Based on averaging over a dozen π-A isotherms, we determined the cross-sectional areas of pure cholesterol to be 38.4, 38.1, and 37.7 Å^2 at surface pressures of 5, 15, and 30 mN/m upon spreading at large areas and slowly compressing (> 4 Å^2/cholesterol molecule/min).

Monolayer compressibilities at the indicated experimental mixing ratios were obtained from π-A data using:

$$C_s = (-1/A)(dA/d\pi) \qquad (3)$$

where A is the area per molecule at the indicated surface pressure and π is the corresponding surface pressure (e.g., Behroozi, 1996). At a given mixing ratio of PC and cholesterol, ideal C_s behavior was determined by apportioning the C_s value for each lipid (as a pure entity) according to both molecular area fraction and mol fraction as described previously (Ali et al., 1994). Thus, at a given constant surface pressure (π),

$$C_s = (1/A)[(C_{s1}A_1)X_1 + (C_{s2}A_2)X_2] \qquad (4)$$

where $X_2 = (1 - X_1)$ and C_s is additive with respect to the product $(C_{si}A_i)$ rather than (C_{si}) for either ideal miscibility or immiscibility. Deviations from additivity of the experimental values indicate nonideal interactions between components in the mixed monolayers. For convenience, we expressed the data in terms of the reciprocal of isothermal compressibility (C_s^{-1}), i.e., surface compressional moduli (Davies and Rideal, 1963), because this facilitated comparisons with bulk elastic moduli of area compressibility measurements made in bilayer systems (e.g., Evans and Needham, 1987; Needham and Nunn, 1990). We used a 100-point sliding window that utilized every 4th point to calculate a C_s^{-1} value before advancing the window one point. Each C_s^{-1} versus average molecular area curve consisted of 200 C_s^{-1} values obtained at equally spaced surface pressures (0.2 mN/m intervals) over the range of 1 to 40 mN/m.

In a recent report in which the π-C_s^{-1} behavior of various pure GalCers, SMs, and PCs was investigated (Smaby et al., 1996a), we discussed the limitations associated with experimentally derived C_s^{-1} values obtained at high surface pressures (>30–35 mN/m). In essence, C_s^{-1} values determined directly from an experimental π-A isotherm display a maximum well below collapse and then diminish at higher surface pressures instead of hyperbolically increasing until film collapse. The C_s^{-1} maximum generally occurs at surface pressures >35 mN/m, but this depends somewhat upon the lipid or lipid mixture under study. Actually, C_s^{-1} values begin to fall away from the expected hyperbolic-like increase before achieving the C_s^{-1} maximum. This behavior is illustrated in Fig. 1. The behavior is highly reproducible and has been attributed to intrinsic experimental factors (e.g., trough composition and/or design) but may also reflect a decrease in lipid film stability at high pressures (e.g., Schwarz et al., 1996). Analogously, the dipole potential (ΔV) versus inverse area behavior (1/A) of various liquid-expanded lipids reportedly is linear up to surface pressures where the second derivative of the π-A isotherms ($d^2\pi/dA^2$) goes from positive to negative values (π_d) (Smaby and Brockman, 1990). The linearity indicates a lack of significant dipole reorientation over the range of surface pressures leading up to π_d and typically encompasses 80–90% of the π-A data for liquid-expanded films. Hence, to improve the C_s^{-1} data at high surface pressures, we fit the experimentally obtained π-A isotherms to the following osmotic-based monolayer equation of state:

$$\pi = (qkT/\omega_1)\ln[(1/f_1)[1 + \omega_1/(A_\pi - \omega_0)]] \qquad (5)$$

where k is Boltzmann's constant, ω_1 is the cross-sectional area of an interfacial water molecule (9.65 $Å^2$), and ω_0 is the cross-sectional area of dehydrated lipid, f_1 is the activity coefficient of interfacial water, and A_π is the total surface area divided by the number of lipid molecules present at a given surface pressure (Wolfe and Brockman, 1988; Smaby and Brockman, 1992; Feng et al., 1994). The scaling parameter q correlates to f_1 and is not unique, but does provide a better fit of the data because it allows for higher-order terms involving the activity coefficient (Smaby and Brockman, 1991b; Feng et al., 1994). Because data obtained near the high- and low-pressure limits often are especially sensitive to the dynamics of the experiment and to trace impurities, respectively (e.g., Middleton and Pethica, 1981), the upper limit for reliable π-A data was defined as the value at which $d^2\pi/dA^2$ goes from positive to negative (typically 10–15% below film collapse) and the lower limit was determined by the molecular area where $\pi = 1.0$ mN/m. From the regions of the π-A experimental data satisfying the preceding criteria, fitted π-A isotherms were generated that provided extrapolated π-A data at high π (approaching film collapse). C_s^{-1} values could then be determined from the extrapolated high pressure data ($\pi \geq 30$ mN/m).

Fig. 1 A illustrates the quality of the curve fitting for pure 16:0–18:1 PC as well as for 16:0–18:1 PC/cholesterol mixtures containing 0.3 or 0.6 mol
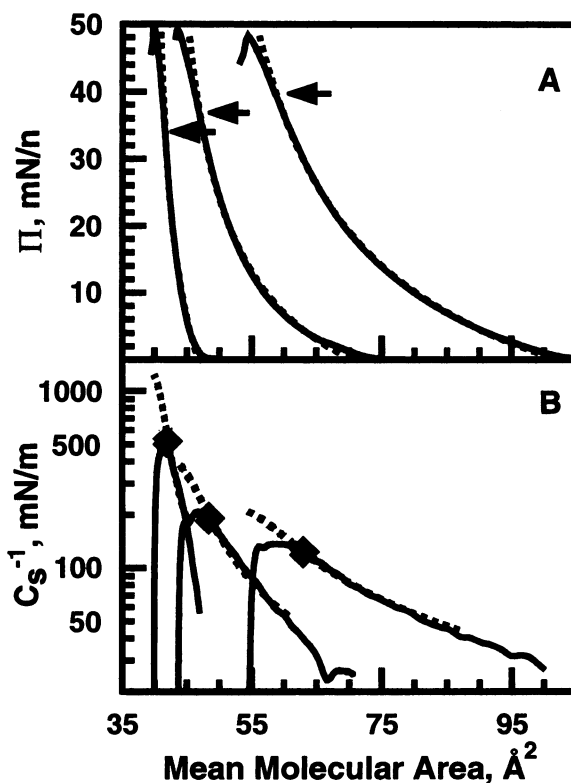

FIGURE 1 Comparison of experimental and fitted isotherms. (A) Surface pressure versus average cross-sectional molecular area (π-A): Experimentally observed isotherms at 0, 0.3, and 0.6 sterol mol fraction mixed with 16:0–18:1 PC (right to left) are represented by the solid lines. Arrows indicate where $d^2\pi/dA^2$ goes from positive to negative. The fitted isotherms (dashed lines) were generated from the experimental isotherms using Eq. 5 as described in Methods. (B) Interfacial elastic modulus of area compressibility (C_s^{-1}) versus average molecular area: C_s^{-1} values were calculated from the experimentally observed π-A isotherms in (A) using the inverse of Eq. 3 as described in the Methods (solid lines). The maximal C_s^{-1} value occurs where $d^2\pi/dA^2$ goes from positive to negative on the corresponding π-A isotherm in (A). The symbol on each curve indicates a surface pressure of 30 mN/m. C_s^{-1} values calculated from the fitted π-A isotherms in (A) (using the inverse of Eq. 3) are shown as dashed lines in (B). Each dashed line in (B) covers the surface pressure range of 6 mN/m to film collapse.

fraction sterol. The dashed lines show the fitted isotherms resulting when the experimental π-A isotherms (solid lines) are fit using Eq. 5. The arrow positioned along each experimental π-A isotherm indicates where $d^2\pi/dA^2$ changes from positive to negative. This change occurs at the same mean molecular area where the C_s^{-1} maximum is observed in the experimentally derived C_s^{-1} versus average area plot (Fig. 1 B, solid lines). The dashed lines in Fig. 1 B correspond to the C_s^{-1} versus average area behavior calculated from the fitted π-A isotherms using the inverse of Eq. 3. The symbols designate the surface pressure of 30 mN/m along each curve in Fig. 1 B. How closely the extrapolated C_s^{-1} values match their experimental counterparts depends on both PC acyl structure and cholesterol content [Table 1; Exptl. C_s^{-1} versus Fitted C_s^{-1} (Calculated)]. The correspondence at 30 mN/m is good, but diminishes at higher surface pressures. The important point is that, regardless of whether one uses the experimental values or the fitted values at 30 mN/m, similar trends are observed in the way that increasing cholesterol affects the different PC molecular species even though the absolute values of the elasticity moduli may differ somewhat (Table 1).

TABLE 1 Cholesterol-induced area condensations and changes in interfacial elastic moduli of area compressibilities

		Area Condensation at 30 mN/m				Elastic Area Compressibility Moduli at 30 mN/m				
		Average Area (Å²/molecule)		Area Condensation			Fitted Exptl. C_s^{-1} (mN/m)			
PC Species	Sterol Mol Fraction	Ideal*	Exptl."	Average (Å²/molec.)◆	Apparent (Å²/PC)◆	Exptl. C_s^{-1} (mN/m)⁼	Ideal**	Calculated"	Total Change in Fitted C_s^{-1} Induced by Sterol (mN/m)◆◆	Change in Fitted C_s^{-1} (mN/m) due to Interaction Nonideality◆◆
di-14:0	0	58	58	0	0	110	118	118	0	0
	0.1	56	52	4	4	110	126	123	5	-3
	0.2	54	47	7	9	123	137	124	6	-13
	0.3	52	43	9	13	208	150	213	95	63
	0.4	50	41	9	15	385	167	462	344	295
	0.5	48	40	8	16	578	191	858	740	667
16:0–18:1	0	63	63	0	0	123	123	123	0	0
	0.1	60	58	2	3	135	130	138	15	8
	0.2	58	53	5	6	159	141	162	39	21
	0.3	55	48	7	11	189	152	200	77	48
	0.4	53	46	7	11	245	170	271	148	101
	0.5	50	44	6	13	346	191	401	278	210
16:0–18:2	0	66	66	0	0	118	121	121	0	0
	0.1	63	60	3	4	130	128	137	16	9
	0.2	60	56	4	5	150	137	158	37	21
	0.3	58	51	7	6	182	151	202	81	51
	0.4	55	48	7	11	238	166	275	154	109
	0.5	52	46	6	12	306	187	387	266	200
16:0–20:4	0	68	68	0	0	108	115	115	0	0
	0.1	64	61	3	4	117	120	119	4	-1
	0.2	61	58	3	5	142	128	144	29	16
	0.3	58	52	6	10	153	141	161	46	20
	0.4	55.5	48.5	6.5	12	181	155	205	90	50
	0.5	53	46	7	14	235	175	274	159	99
16:0–22:6	0	70	70	0	0	106	108	108	0	0
	0.1	67	64	3	3	112	115	115	7	0
	0.2	64	61	3	3	125	123	132	24	9
	0.3	60	55	5	8	140	131	153	45	22
	0.4	57	51	6	10	173	145	198	90	53
	0.5	54	48	6	12	214	164	247	139	83
di-18:1	0	66	66	0	0	116	120	120	0	0
	0.1	63	62	1	1	130	127	134	14	7
	0.2	60	57	3	4	148	136	151	31	15
	0.3	58	53	5	6	169	149	179	59	30
	0.4	55	49	6	9	200	164	220	100	56
	0.5	52	46	6	12	253	185	294	174	109
di-18:2	0	70	70	0	0	116	123	123	0	0
	0.1	67	64	3	3	128	131	135	12	4
	0.2	64	61	3	3	143	140	154	31	14
	0.3	60	54	6	9	163	149	183	60	34
	0.4	57	51	6	10	191	165	224	101	59
	0.5	53.5	47.5	6	13	239	186	311	188	125
di-20:4	0	72	72	0	0	105	111	111	0	0
	0.1	69	66	3	3	112	118	117	6	-1
	0.2	65	61	4	5	122	125	125	14	0
	0.3	62	57	5	7	130	136	136	25	0
	0.4	58	52	6	10	145	147	153	42	6
	0.5	55	48.5	6.5	13	173	167	183	72	16
di-22:6	0	75	75	0	0	94	98	98	0	0
	0.1	71	69	2	3	101	103	105	7	2
	0.2	68	64	4	4	108	111	111	13	0
	0.3	64	59	5	7	113	119	117	19	-2
	0.4	60	54	6	10	125	129	128	30	-1
	0.5	56	50	6	13	147	144	146	48	2

*Calculated using Eq. 1.
"Determined from π-A isotherms.
◆Ideal minus exptl. average area.
◆Calculated using Eq. 2.
⁼Calculated from π-A isotherms using Eq. 3.
**Determined by fitting the π-A isotherms of the pure lipids using Eq. 5 and applying Eq. 3 and Eq. 4.
"Determined by fitting π-A isotherms using Eq. 5 and applying Eq. 3.
◆◆Calculated C_s^{-1} of mix minus calculated C_s^{-1} of pure PC.
◆◆Calculated C_s^{-1} minus ideal C_s^{-1}.

RESULTS

Because the bulk of PC in most tissues has saturated sn-1 acyl and unsaturated sn-2 chains, our initial focus was on PCs with this structural motif. However, we also investigated the interactions of cholesterol with di-unsaturated PCs because of their involvement in important cellular processes. For instance, during cold acclimation, the proportion of di-unsaturated species of PC and PE in plants increases by 50% while sterol concentration increases only slightly (Steponkus et al., 1995, and references therein). Also, aside from being important in the normal generation of various saturated sn-1, unsaturated sn-2 PCs, di-unsaturated PCs such as di-20:4 PC appear to be produced during the reuptake of liberated arachidonate following stimulation by ionophores and to play a role in the production of the cannabinoid receptor agonist, N-arachidonoylethanolamine, also known as ananadamide (Kuwae et al., 1997, and references therein).

Interfacial elastic moduli of area compressibility of di-14:0 PC/cholesterol mixtures

Because much earlier work had been carried out with PCs containing di-saturated acyl chains, we included a representative fluid-phase PC with this structural motif (e.g., di-14:0 PC = 1,2-dimyristoyl-sn-glycero-3-phosphocholine) as a standard to compare against PCs containing one or two unsaturated acyl chains. Fig. 2 shows the surface pressure versus average molecular area (π-A) behavior for various di-14:0 PC/cholesterol mixtures (Fig. 2 A) from which the C_s^{-1} versus average molecular area behavior was determined (Fig. 2 B). The higher the C_s^{-1} value, then the lower the interfacial elasticity. The C_s^{-1} versus average molecular area plots at each mixing ratio begin at 1 mN/m and end at 40 mN/m with the intervening symbols designating 5, 15, and 30 mN/m, respectively, as molecular area decreases. The data depicted by the solid lines were derived directly from experimental π-A isotherms, whereas the dashed portion of a curve represent extrapolated data obtained by fitting the experimental data as described in Methods.

In the case of di-14:0 PC, the pure lipid is chain-disordered, i.e., liquid-expanded, at all surface pressures below film collapse at 24°C (Fig. 2 A). The C_s^{-1} value (118 mN/m) at 30 mN/m reflects the fluid nature of the lipid packing state (Table 1). Interestingly, as increasingly more cholesterol is mixed with di-14:0, the average molecular area decreases while the in-plane elasticity is relatively unaffected until a critical sterol concentration is reached (Fig. 2 and Table 1). Thereafter, further increases in cholesterol result in dramatic increases in C_s^{-1}. The sterol concentration at which the dramatic increase in C_s^{-1} begins is dependent upon surface pressure. For instance, C_s^{-1} values are quite similar for mixed films containing cholesterol mol fractions up to 0.4 at low surface pressures (e.g., 5 mN/m). In contrast, at high surface pressures in the range thought to mimic biological membranes (e.g., $\pi \geq 30$
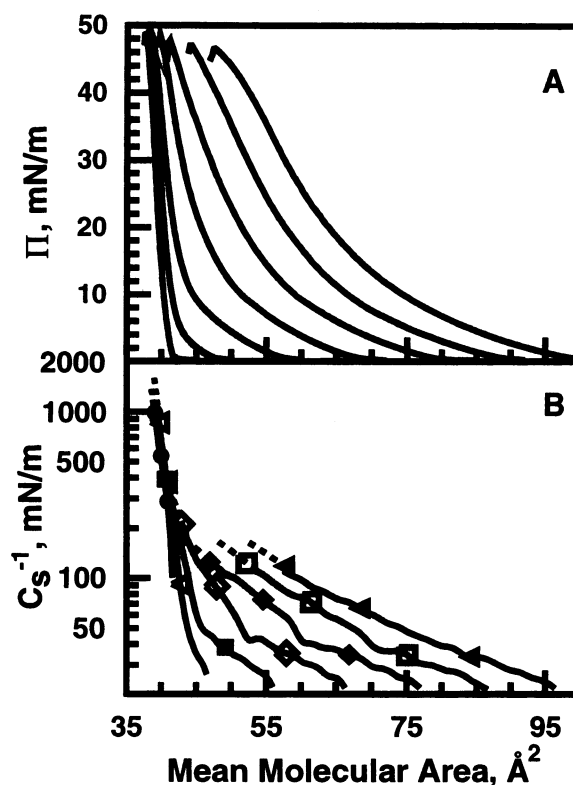

FIGURE 2   di-14:0 PC/cholesterol mixed monolayers. Data were collected using an automated Langmuir-type film balance as described in Methods. (A) Surface pressure versus average cross-sectional molecular area: isotherms (from right to left) contain 0, 0.1, 0.2, 0.3, 0.4, 0.5, and 0.6 mol fraction sterol. (B) Interfacial elastic modulus of area compressibility (C_s^{-1}) versus average molecular area: curves at each mixing ratio begin at 1 mN/m and end at 40 mN/m (from right to left) with the intervening symbols designating 5, 15, and 30 mN/m, respectively, as the average molecular area decreases. Solid lines indicate experimental observations; dashed lines indicate extrapolated behavior based on fitting. Cholesterol mol fractions are indicated by the following symbols: X_{chol} of 0 = (▲); of 0.1 = (□); of 0.2 = (◆); of 0.3 = (◇); of 0.4 = (■); of 0.5 = (△); and of 0.6 = (●).

mN/m), di-14:0 PC can only accommodate cholesterol mol fractions up to or slightly above 0.2 before the interfacial elasticity begins to change. Further elevation of sterol results in an abrupt decrease in interfacial elasticity such that 6- to 7-fold higher C_s^{-1} values are achieved when X_{chol} reaches 0.5 (Fig. 2 and Table 1).

Interfacial elastic moduli of area compressibility of 16:0-18:1 PC/cholesterol mixtures

To determine whether similar trends occur when a single cis double bond is in the middle of the sn-2 acyl chain, we analyzed the C_s^{-1} versus average molecular area behavior of 1-palmitoyl-2-oleoyl-sn-glycero-3-phosphocholine (16:0-18:1$^{\Delta9(c)}$ PC) and cholesterol mixtures (Fig. 3 B). The π-A isotherms for the mixtures are shown in Fig. 3 A. As with di-14:0 PC, pure 16:0-18:1 PC is chain-disordered, i.e., liquid-expanded, at all surface pressures below film
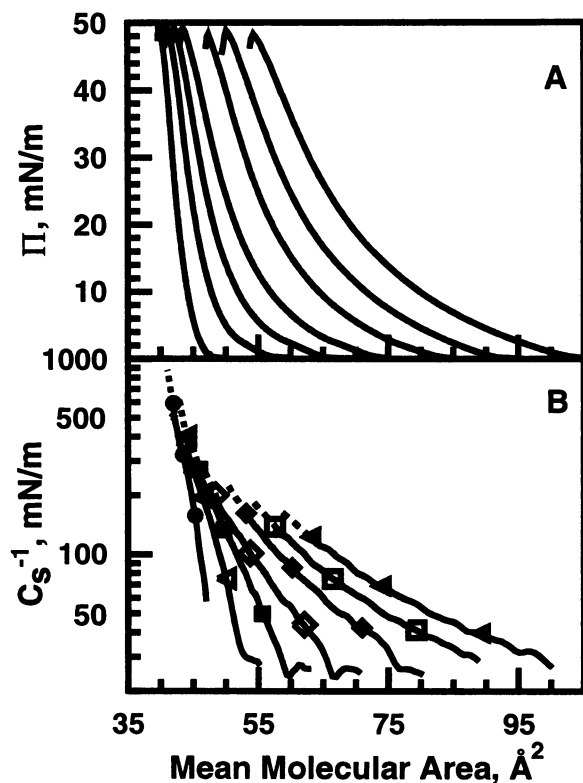
FIGURE 3   16:0–18:1 PC/cholesterol mixed monolayers. (Other details same as in Fig. 2 legend.)

collapse at 24°C (Smaby et al., 1996a, and references therein). Not surprisingly, the C_s^{-1} value (123 mN/m) 16:0–18:1 PC at 30 mN/m reflects its fluid nature despite being 5 Å²/molecule larger than di-14:0 PC (Table 1). Interestingly, at 30 mN/m, the response of 16:0–18:1 PC to increasing cholesterol concentrations differs somewhat from that of di-14:0. Rather than accommodating low mol fractions of cholesterol (X_{chol} < 0.2) without affecting in-plane elasticity, 16:0–18:1 PC shows steadily increasing C_s^{-1} values over this same sterol concentration range. Yet, at X_{chol} of 0.3, the C_s^{-1} value reaches 200 mN/m, a value very similar to that observed with di-14:0 PC (213 mN/m) (Fig. 3 B; Table 1). Moreover, as the cholesterol content increases further (0.2 < X_{chol} < 0.6), the in-plane elasticity of the 16:0–18:1 PC/sterol mixtures continues to decline steadily, but not as steeply as with di-14:0 PC/sterol mixtures. The end result is about a 3-fold decrease in the in-plane elasticity at X_{chol} of 0.5 compared to pure, fluid-phase 16:0–18:1 PC (Table 1). Hence, relative to the changes observed in di-14:0 PC at high sterol mol fractions, 16:0–18:1 PC "buffers" the ability of cholesterol to lower the in-plane elasticity.

Interfacial elastic moduli of area compressibility of sn-1 saturated, sn-2 polyunsaturated PC/cholesterol mixtures

To determine how multiple cis unsaturation in the sn-2 chain of PC affects the ability of cholesterol to decrease

in-plane elasticity, we next investigated mixtures of cholesterol and 1-palmitoyl-2-linoleoyl-sn-glycero-3-phosphocholine (16:0–18:2$^{\Delta9,12(c)}$ PC), 1-palmitoyl-2-arachidonoyl-sn-glycero-3-phosphocholine (16:0–20:4$^{\Delta4,7,10,13(c)}$ PC) or 1-palmitoyl-2-docosahexenoyl-sn-glycero-3-phosphocholine (16:0–22:6$^{\Delta4,7,10,13,16,19(c)}$ PC) (Figs. 4 B, 5 B, and 6 B, respectively). The π-A isotherms are shown in Figs. 4 A, 5 A, and 6 A. Each of these PCs displayed chain-disordered, i.e., liquid-expanded, at all surface pressures below film collapse at 24°C. As with di-14:0 PC and 16:0–18:1 PC, the C_s^{-1} values at 30 mN/m were rather similar despite the fact that the cross-sectional molecular areas increased slightly as the unsaturation level of the sn-2 chain increased (Table 1).

In the high pressure region (e.g., 30 mN/m), increasing the cholesterol content of the PC/sterol films resulted in steadily increasing C_s^{-1} values. Overall, the presence of highly unsaturated sn-2 chains in PC resulted in cholesterol-induced liquid-ordered states with similar in-plane elasticities but at larger average molecular areas than those in di14:0 PC/cholesterol mixtures. Yet, both the degree of unsaturation and the location of the cis double bonds in the sn-2 chain did affect the magnitude of the cholesterol-induced increases in C_s^{-1} (Table 1). For instance, the C_s^{-1} values observed for 16:0–18:2$^{\Delta9,12(c)}$ PC were very similar to those of 16:0–18:1$^{\Delta9(c)}$ PC at equivalent sterol mol fractions of 0.3 or 0.5 (Table 1). This indicates that locating a second cis double bond at a hydrocarbon position where the associated crankshaft-type tg⁻ kink is not adjacent to the
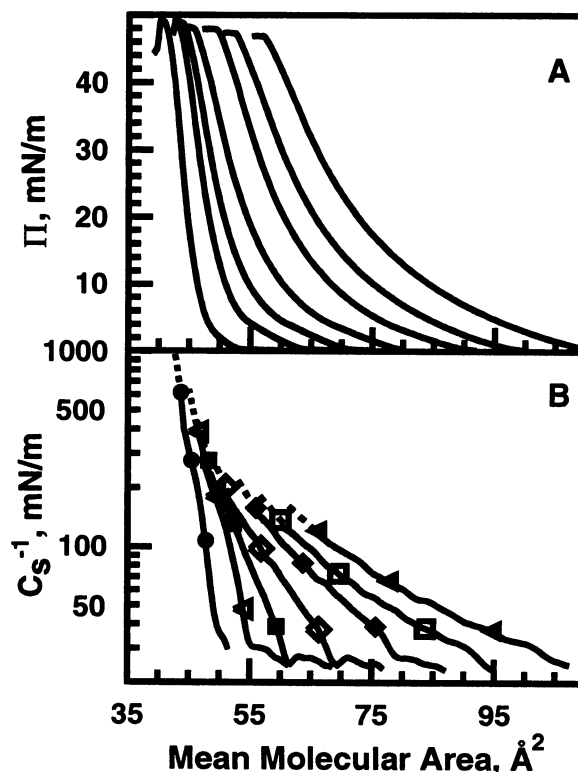

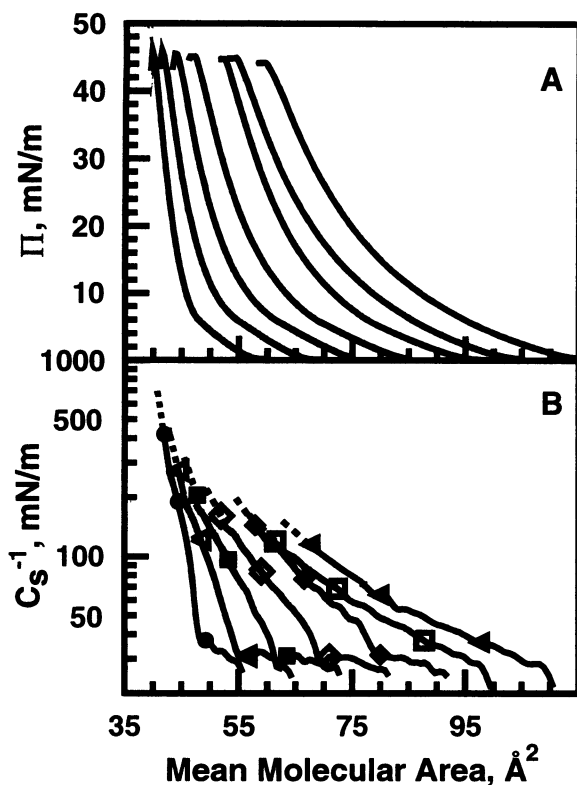FIGURE 4   16:0–18:2 PC/cholesterol mixed monolayers. (Other details same as in Fig. 2 legend.)

FIGURE 5   16:0–20:4 PC/cholesterol mixed monolayers. (Other details same as in Fig. 2 legend.)

FIGURE 6   16:0–22:6 PC/cholesterol mixed monolayers. (Other details same as in Fig. 2 legend.)

planar steroid ring enhances the ability of cholesterol to change the in-plane elasticity of the system. In the case of 16:0–20:4$^{\Delta 4,7,10,13(c)}$ PC and 16:0–22:6$^{\Delta 4,7,10,13,16,19(c)}$ PC, the additional unsaturation at carbon positions that produce crankshaft-type tg^{-} kink(s) within the hydrocarbon region adjacent to the planar steroid ring significantly interferes with cholesterol reducing the in-plane elasticity of these PCs (Table 1). Yet, the fact that the cholesterol-induced C_s^{-1} values in the sterol/16:0–22:6 PC mixtures, where cis double bonds occur all along the sn-2 chain, are slightly lower than those of the sterol/16:0–20:4 PC mixtures indicates that cholesterol's side chain is responsible for a small contribution to the observed change in the in-plane elasticity (Table 1).

Over the low-surface-pressure region ($\pi < 14$ mN/m), increasing cholesterol content produced marked breaks in the slopes of the C_s^{-1} versus average area plots (Figs. 4 B, 5 B, and 6 B). The surface pressures at which the breaks occurred increased as the sn-2 chain unsaturation increased (e.g., note positions of 5 mN/m symbols in relation to breaks in slope). The end result was that, at low surface pressure (e.g., 5 mN/m), cholesterol mol fractions up to 0.4 had little effect on C_s^{-1} values of 16:0–18:2 PC. Above 0.4 mol fraction sterol, the low pressure C_s^{-1} values began to rise steeply. In this respect, the behavior of 16:0–18:2 PC and 16:0–18:1 PC were similar. In contrast, C_s^{-1} values for 16:0–20:4 PC and 16:0–22:6 PC actually decreased slightly
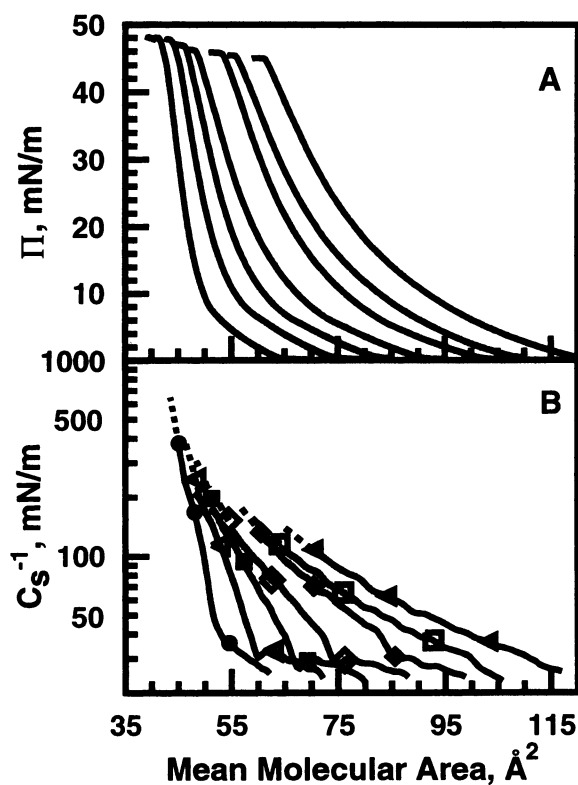
over the low pressure region at cholesterol mol fractions between 0 and 0.2 and then remained relatively constant until cholesterol mol fractions exceeded 0.5 (Figs. 5 B and 6 B).

Interfacial elastic moduli of area compressibility of di-unsaturated PC/cholesterol mixtures

To determine whether the cholesterol-induced changes in interfacial elasticity were affected further when both PC acyl chains are unsaturated, we investigated the behavior of cholesterol and dioleoyl-sn-glycero-3-phosphocholine (di-18:1$^{\Delta 9(c)}$ PC), dilinoleoyl-sn-glycero-3-phosphocholine (di-18:2$^{\Delta 9,12(c)}$ PC), diarachidonoyl-sn-glycero-3-phosphocholine (di-20:4$^{\Delta 5,8,11,14(c)}$ PC, or didocosahexenoyl-sn-glycero-3-phosphocholine (di-22:6$^{\Delta 4,7,10,13,16,19(c)}$ PC) (Figs. 7–10, respectively).

In their pure state, di-18:1 PC, di-18:2 PC, di-20:4 PC, and di-22:6 PC were liquid-expanded at all surface pressures below film collapse. Their C_s^{-1} values at 30 mN/m were 120, 123, 111, and 98 mN/m at molecular areas of 66, 70, 72, and 75 Å^2/molecule, respectively (Table 1). Examination of Figs. 7–10 reveals that substitution of the unsaturated chain for palmitate at the sn-1 position generally mitigates the ability of cholesterol to elevate the C_s^{-1} values and results in slightly larger areas at matching sterol mol fractions (Table 1). As a result, C_s^{-1} values were ~25% lower when both chains were unsaturated and, the more
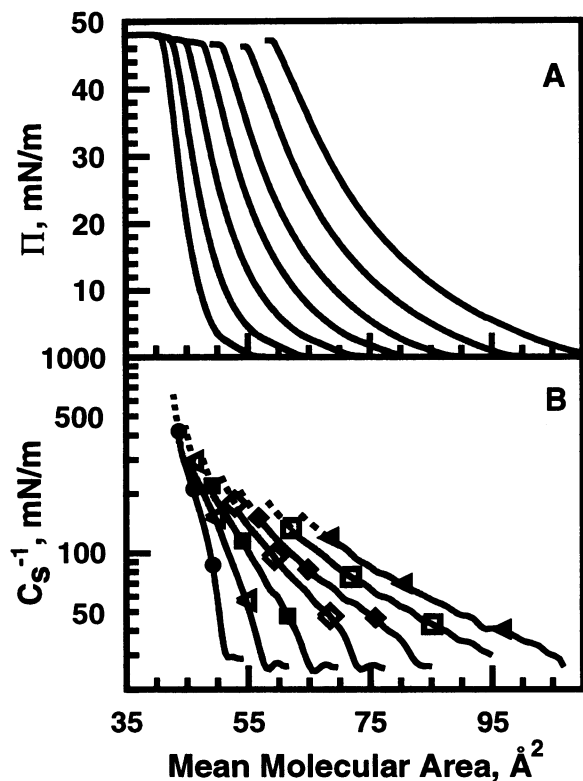
FIGURE 7 Di-18:1 PC/cholesterol mixed monolayers. (Other details same as in Fig. 2 legend.)
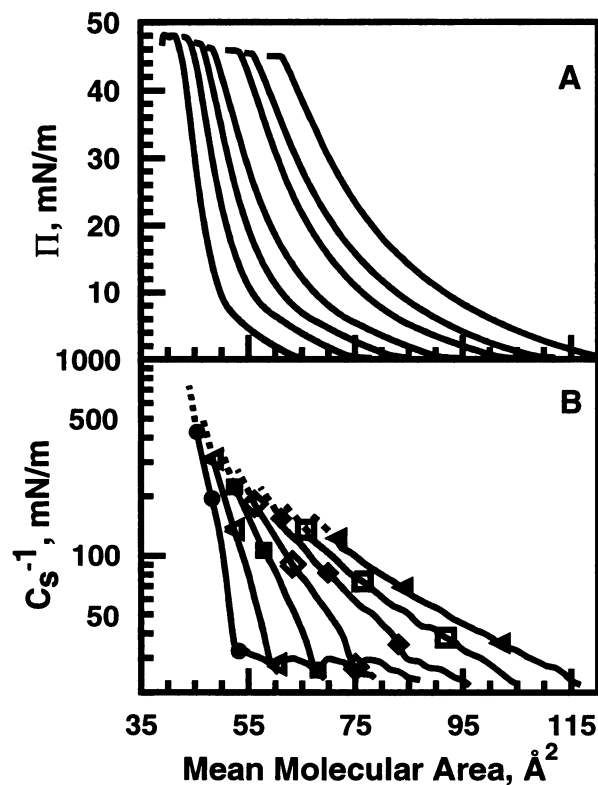
FIGURE 8 Di-18:2 PC/cholesterol mixed monolayers. (Other details same as in Fig. 2 legend.)

unsaturated the acyl chains, then the better the PC/sterol mixtures could maintain relatively high in-plane elasticity and larger average molecular areas in the presence of high sterol concentrations.

Compared to their sn-1 saturated counterparts, the cholesterol-induced changes in the in-plane elasticity of the di-unsaturated PCs deviated less from ideal additivity (Table 1). However, among the di-unsaturated PCs, those with the highest unsaturation levels exhibited cholesterol-induced C_s^{-1} values that were closest to ideal additivity. Such behavior is consistent with a lack of interaction between highly unsaturated PCs (e.g., di-22:4 PC and di-22:6 PC). Also, as observed with the sn-1 saturated, sn-2 unsaturated PCs (Figs. 3 B, 4 B, 5 B, and 6 B) over the low surface pressure region (π < 14 mN/m), increasing cholesterol content produced marked breaks in the slopes of the C_s^{-1} versus average area plots of the di-unsaturated PCs (Figs. 7 B, 8 B, 9 B, and 10 B). The surface pressures at which the breaks occurred tended to increase with increasing unsaturation of the sn-2 chain (e.g., note positions of 5 mN/m symbols in relation to breaks in slope).

Comparison of the cholesterol-induced changes in interfacial elastic packing and in the area condensations of sterol/PC mixtures

Because many previous investigators had relied on area condensation measurements in their attempts to determine

how the structural features of the PC hydrocarbon region modulate interaction with cholesterol (see Discussion), we compared area condensations with the C_s^{-1} values under identical monolayer conditions. The results in Table 1 summarize the values obtained at 30 mN/m which mimic the conditions of biomembranes. The exact value within the high surface pressure region at which bilayers and monolayers are in equilibrium remains a subject of much debate (e.g., Phillips and Chapman, 1968; Demel et al., 1975; Hui et al., 1975; Evans and Waugh, 1977; Blume, 1979; MacDonald and Simon, 1987; Osborn and Yager, 1995; Marsh, 1996, and references therein).

The left panels of Table 1 show the data analyzed in terms of the cross-sectional area changes induced by equimolar cholesterol and were derived by compiling earlier (Smaby et al., 1994; 1997) and new results. Close inspection reveals that the magnitude of cholesterol-induced area condensations can be similar even though the molecular packing densities of the various PCs may differ before and after mixing with cholesterol. The data also clearly show that varying the cis unsaturation level and position in the sn-2 chain of PCs or replacing saturated chains with unsaturated ones in the sn-1 position produces no strong correlations among the area condensations induced by cholesterol at 30 mN/m.

In contrast, the results in Table 1 clearly show that changes in the C_s^{-1} values induced by cholesterol are very responsive to subtle structural and configurational features
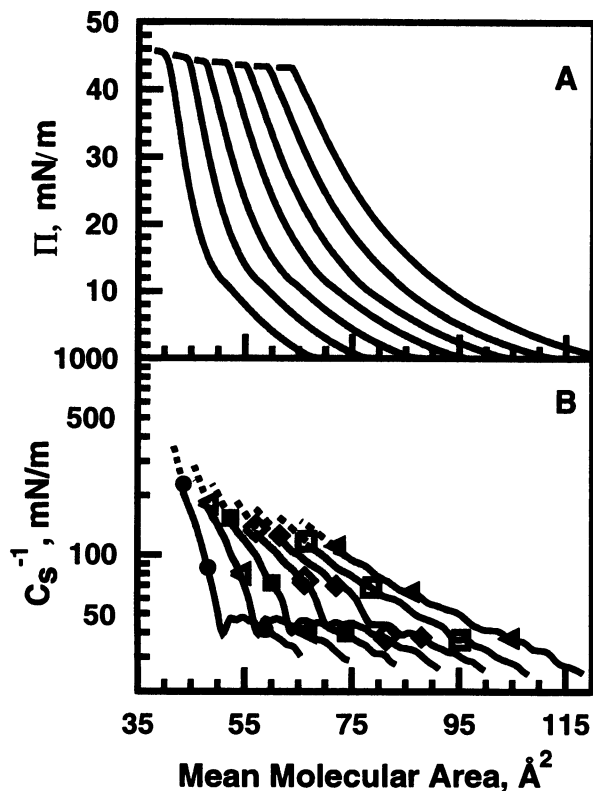
FIGURE 9   Di-20:4 PC/cholesterol mixed monolayers. (Other details same as in Fig. 2 legend.)
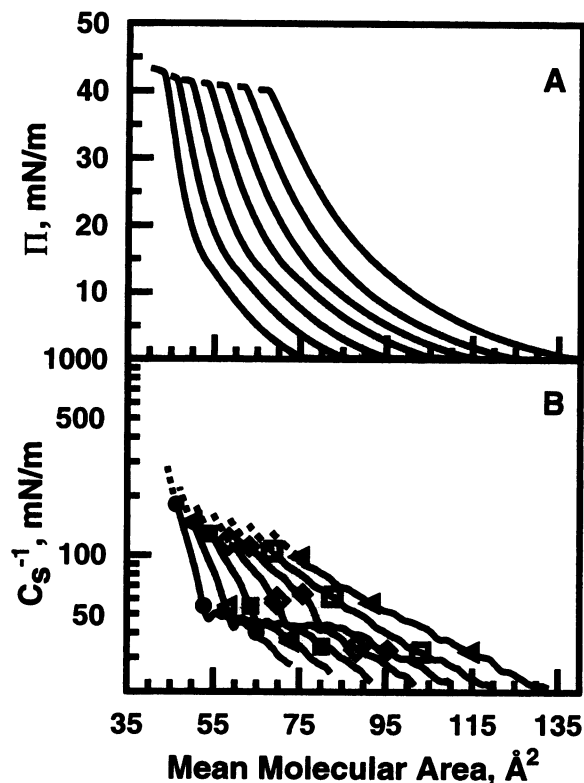
FIGURE 10   Di-22:6 PC/cholesterol mixed monolayers. (Other details same as in Fig. 2 legend.)

of the PC acyl chains including the degree of unsaturation in each acyl chain as well as the distribution of *cis* double bonds in the acyl chain(s). Notably, the largest decrease in interfacial elasticity induced by cholesterol (6- to 7-fold) among the various fluid-phase PCs occurs when both acyl chains are saturated. In contrast, when both acyl chains have multiple *cis* double bonds along each acyl chain, cholesterol decreases the elasticity of the films more modestly but significantly (1.7-fold). Even so, most of this latter cholesterol-induced change occurs by virtue of the sterol itself being a smaller and more rigid molecule than the PC. At matching sterol mol fractions, the ideal and calculated C_s^{-1} values are quite similar and their differences (change in fitted C_s^{-1} due to interaction nonideality) are relatively small when both PC acyl chains are highly unsaturated (Table 1).

DISCUSSION

The results of this study clearly show that measurements of the interfacial elastic moduli of area compressibility (C_s^{-1}) provide a valuable means to quantitatively assess the impact of cholesterol on the in-plane elastic packing interactions in phosphoglyceride-cholesterol mixed monolayers. While the basic approach has been utilized on occasion to help construct phase diagrams of di-16:0 PC/cholesterol and di-14:0 PC/cholesterol mixed monolayers (Albrecht et al., 1981;

Hirshfeld and Seul, 1990), we are unaware of previous monolayer studies in which rigorous and comprehensive C_s^{-1} analyses have been used to address the effects of phosphoglyceride acyl structure on interactions with sterols. Instead, investigators have usually focused on cross-sectional area condensations induced by cholesterol in their attempts to assess the role that acyl structure might play in modulating sterol-phosphoglyceride interactions. This emphasis on area condensations has been useful but has not provided a completely coherent and self-consistent picture. What is clear is that the headgroup and hydrocarbon composition of phosphoglycerides and sphingolipids do influence the magnitude of the cross-sectional area changes induced by cholesterol (Phillips, 1972; Smaby et al., 1994; 1996b and references therein). In general, maximal cholesterol-induced area condensations occur when phosphoglycerides are fluid-phase before mixing with cholesterol (Phillips, 1972). What has remained controversial is whether the magnitude of cholesterol-induced area condensations of PCs respond in a straightforward manner to changing levels and positions of *cis* double bonds along the acyl chain(s). For instance, Chapman et al. (1969) investigated the mixing of cholesterol with either $18{:}0{-}18{:}1^{\Delta 9}$ PE or $18{:}0{-}18{:}1^{\Delta 6}$ PE at 20 mN/m and concluded that the position of *cis* double bonds in unsaturated phospholipids was not important for condensation effects. In contrast, Demel et al. (1972) concluded that the magnitude of the cholesterol-induced area condensation measured in sterol/PC films does

depend upon the unsaturation level and the distribution of double bonds in the acyl chains based on studies of equimolar cholesterol and PCs with acyl chains containing one to six *cis* double bonds at 12 mN/m. Moreover, the area condensations induced by high levels of cholesterol (X_{chol} of 0.5) reportedly diminished when both PC acyl chains contain *cis* double bonds. In subsequent monolayer studies of PCs with various acyl structures (including branched and unsaturated chains), the cholesterol-induced area changes at 5 mN/m observed by Tinoco and colleagues supported the results of Demel et al. (1972) while measurements at surface pressures that mimic biological membranes did not (Ghosh et al., 1973; Evans et al., 1987). At the higher surface pressure (40 mN/m), no strong correlation was observed between double bond position and the magnitude of cholesterol-induced area condensation in agreement with our findings (Fig. 11).

Recent studies involving the cholesterol-induced area condensations of PCs with highly unsaturated acyl chains also have proven to be controversial. Parks and Thuren (1993) noted that the cholesterol-induced area condensations of 16:0–18:1 PC and 16:0–20:5 PC at 25 mN/m were similar, but were not as high as that of 16:0–22:6 PC at

sterol mol fractions between 0.15 and 0.5. In contrast, Zerouga et al. (1995) reported that 18:0–22:6 PC is not condensed at all by cholesterol ($0.2 \leq X_{chol} \leq 0.5$) at surface pressures of 10, 20, or 25 mN/m. While some of these discrepancies probably have arisen for technical reasons such as differences in monolayer trough calibration, failure to accurately quantitate the lipid components, and oxidation of cholesterol or the polyunsaturated PCs, we believe that many of the differences are simply due to the complex and nonlinear effect that surface pressure has on the magnitude of the cholesterol-induced area condensations that occur in PCs containing *cis* unsaturated acyl chains.

To illustrate how the surface pressure influences the magnitude of cholesterol-induced condensations, we have plotted the apparent area condensation per PC molecule as a function of surface pressure at equimolar cholesterol (Fig. 11). Expressing the data in this manner portrays the area condensation solely in terms of change to the PC molecule (e.g., Lund-Katz et al., 1988; Smaby et al., 1994; 1996b). From the data, it is clear that surface pressure influences the apparent area condensations of PC species containing *cis* unsaturated acyl chains in complex ways. They do not simply increase as the surface pressure decreases but show maxima between 2 and 17 mN/m depending upon the degree of acyl unsaturation. After reaching their maxima, the apparent area condensations tend to converge so that by 30 mN/m, seven of the nine PC species are within 3 or 4 $Å^2$/molecule of each other. The paths toward convergence often cross over one another rendering any comparison of the different PC species very much dependent upon surface pressure, especially when $\pi < 17$ mN/m. Hence, whether area condensation data obtained at low pressures provide accurate insights into lipid structural features that modulate sterol-PC interactions in biomembranes is questionable.

As alluded to above, the lack of strong correlation between PC acyl structure and cholesterol-induced area condensation at 30 mN/m (Table 1) is probably due to the complex nature of the area condensation event. For instance, the bulk of the cholesterol-induced area condensation of fluid-phase PCs derives from the acyl ordering attained when *trans-gauche* isomerization about the carbon-carbon bonds is reduced. However, the "baseline" order of the saturated sn-1 chain is not necessarily identical in all fluid-phase PCs and depends upon the unsaturation level of the sn-2 chain (e.g., Feng and MacDonald, 1995). The presence of highly unsaturated sn-2 chains has a disordering effect on the adjacent saturated sn-1 chains of PCs (Holte et al., 1995; 1996). Hence, in this situation, a greater contribution from the sn-1 chain to the area condensation would be expected compared to the contribution of the sn-1 chain in di-saturated PCs. Also, area condensation by sterol can result from processes other than alteration of the intramolecular acyl chain order. Cholesterol may also change the observed average molecular area by changing the average molecular tilt of certain PC species [(e.g., Smaby et al. (1996b)]. Considering the various processes that can con-
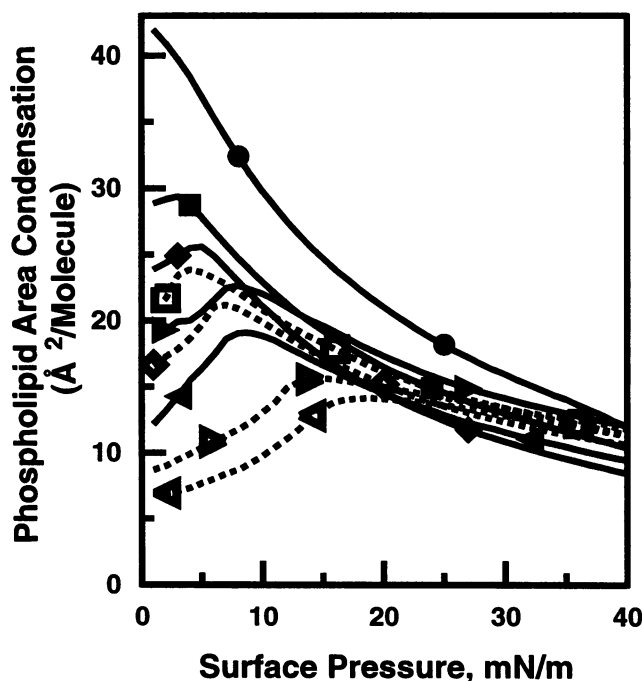

FIGURE 11   Apparent phosphatidylcholine molecular area condensation versus surface pressure at equimolar cholesterol. Each line represents the cholesterol-induced area condensation expressed as the area change imparted to a given PC species and calculated using Eq. 2 of Methods at 1 mN/m intervals over the surface pressure range from 1 to 40 mN/m at 24°C. Solid lines represent PCs in which at least one acyl chain is saturated (e.g., myristate or palmitate). Dashed lines represent PCs in which neither acyl chain is saturated. PC molecular species are indicated by the following symbols: di-14:0 PC = (●); 16:0–18:1 PC = (■); 16:0–18:2 PC = (♦); 16:0–20:4 PC = (▶); 16:0–22:6 PC = (◀); di-18:1 PC = (□); di-18:2 PC = (◇); di-20:4 PC = (▷); di-22:6 PC = (◁).

tribute to area condensation and that the precision of the molecular area measurement at high surface pressures may produce differences (generally, 1 to 2 Å^2 per molecule) that are insufficient to unequivocally discriminate among certain subtle structural features of fluid-phase PCs, conclusions based solely on this approach must be viewed with caution.

Because we wished to focus on conditions thought to mimic biomembranes (e.g., $\pi \geq 30$ mN/m), we sought an alternative and more sensitive means to determine how structural changes imparted to the acyl chains of phosphoglycerides and sphingolipids during the course of physiological remodeling might affect the interactions of these lipids with cholesterol. To this end, we analyzed the elastic moduli of area compressibility (C_s^{-1}) to achieve the desired insights into how the level and position of cis double bonds in the sn-2 chain of PCs containing saturated sn-1 chains influence interactions with cholesterol. Expressing the data as C_s^{-1}, which is the inverse of the lateral compressibility moduli, is convenient because it facilitates comparisons with area dilation, i.e., elastic moduli of area compressibility measurements, made in bilayer vesicles (e.g., Evans and Needham, 1987; Needham and Nunn, 1990). However, as noted in our recent monolayer study of the elastic packing interactions of various pure sphingolipids and select PCs with saturated or monounsaturated acyl chains (Smaby et al., 1996a), it must be stressed that the in-plane area elasticity moduli obtained for bilayers using the micropipette aspiration does include a small contribution from the bending or curvature moduli (Evans and Rawicz, 1990). While this latter parameter dominates when applied tensions are low (2–3 × 10^{-3} mN/m), its contribution, albeit small, still persists when applied tensions are elevated (2 to 3 orders of magnitude) to conditions where the area dilation behavior dominates.

Among the PC species we investigated here, cholesterol-induced packing states with the lowest in-plane elasticity occurred when both acyl chains were saturated. With fluid-phase di-14:0 PC, the C_s^{-1} value increased over 7-fold upon mixing with equimolar cholesterol. It is clear that the reduction in the in-plane elasticity induced by equimolar cholesterol is not due solely to the sterol being smaller and more rigid than the PC. This is evident from the data in Table 1 showing the changes in the fitted experimental C_s^{-1} values due to interaction nonideality. The results are consistent with recent energy minimization computations depicting cholesterol making van der Waals contacts with both of the acyl chains of di-14:0 PC (Vanderkooi, 1994).

Introduction of a single cis double bond between carbons 9 and 10 of the sn-2 chain of PC has dramatic effects on the ability of equimolar cholesterol to decrease film elasticity. Instead of the 7.5-fold change in C_s^{-1} value observed in di-14:0 PC, the cholesterol-induced decrease in interfacial elasticity for 16:0–18:1 PC was only 3.5-fold, even though the fluid-phase C_s^{-1} values of the two PCs in the absence of cholesterol were very similar (Table 1). Using the micropipette aspiration approach, which requires bilayer vesicles to be relatively stable, Needham et al. (1988) reported a 5-fold

decrease in bilayer area compressibility for di-14:0 PC/cholesterol (1:1) compared to fluid-phase di-14:0 PC vesicles, but recent measurements have resulted in much greater cholesterol-induced changes (Needham, 1995). However, when 50 mol % cholesterol was mixed with 18:0–18:1 PC, a 4-fold increase in the elastic area expansion modulus of bilayer vesicles was observed (Needham and Nunn, 1990).

Introduction of a second cis double bond into the middle area of the sn-2 acyl chain (e.g., 16:0–18:2 PC) reduced the C_s^{-1} value in equimolar mixtures with sterol only slightly compared to the 16:0–18:1 PC/sterol equimolar mixtures. However, addition of more cis double bonds at sn-2 acyl positions closer to the polar headgroup (16:0–20:4$^{\Delta 5,8,11,14(c)}$ PC) or at positions interspersed all along the sn-2 acyl chain (e.g., 16:0–22:6$^{\Delta 4,7,10,13,16,19(c)}$ PC) further mitigated the ability of cholesterol to reduce film interfacial elasticity. Hence, although significant changes in the in-plane elasticity were induced by cholesterol in all PCs that had at least one saturated acyl chain, the level and position of cis double bonds in the sn-2 acyl chain appear to strongly modulate the elasticity of the films. Most likely, this behavior reflects the diminished capacity of the α surface of the rigid steroid ring to interact with unsaturated sn-2 chains because of the "kinks" introduced by the cis double bonds, which limit the favorable van der Waals interactions. In this respect, the location of the cis double bond(s) appears to be critical because significant changes in the in-plane elasticity of di-18:1$^{\Delta 9(c)}$ PC and di-18:2$^{\Delta 9,12(c)}$ PC were evident and the bulk of the changes could not be attributed to cholesterol being a small, relatively rigid molecule. This indicates that that the rigid sterol ring can still exert significant effects if the cis double bond(s) are located at positions that do not interfere with van der Waals contacts (e.g., Stillwell et al., 1996, and references therein). Only in the case of PCs with highly unsaturated acyl chains (e.g., di-20:4 PC and di-22:6 PC) can the changes induced by cholesterol be attributed almost entirely to sterol rigidity in and of itself. In other cases, the in-plane elasticity induced by cholesterol is significantly lower than predicted by simple additivity.

Finally, examination of the C_s^{-1} versus average molecular area plots (Figs. 3–10) reveals a marked discontinuity in the slope within the low pressure range ($\pi \leq 14$ mN/m) at certain mol fractions of cholesterol. Each PC species shows evidence of the discontinuity, but they are most striking in PCs containing more than one cis double bond in an acyl chain. These discontinuities probably define low pressure phase boundaries and may involve domain organizational changes that can be visualized by fluorescence microscopy. Indeed, the size and shape of fluorescent PC domains that form in di-14:0 PC/cholesterol (7:3) mixed monolayers change markedly over the surface pressure range of 5 to 14 mN/m (Subramaniam and McConnell, 1987; Hirshfeld and Seul, 1990). Yet, at a constant surface pressure, metastable domain structures with equilibrium times of days or weeks can occur as a result of favorable domain "edge energy," i.e., when a balance occurs between

line tension and dipolar electrostatic forces (McConnell, 1996; McConnell and Koker, 1996). Hence, the interactions that occur between cholesterol and PC within the low pressure phases may differ considerably from what occurs at membrane-like higher pressures. Interestingly, Fig. 12 shows that plotting the surface pressure eliciting maximum area condensation (from Fig. 11) versus the surface pressure of the C_s^{-1} transition discontinuity (from Figs. 3–10) for the PC unsaturated species mixed with equimolar sterol reveals a strong correlation (correlation coefficient $= 0.990$) between these parameters.

Implications

The fact that the magnitude of the cholesterol-induced reduction in in-plane elasticity is so responsive to the acyl structure and configuration in PC, in many ways, is consistent with previous calorimetric studies involving cholesterol and PCs with unsaturated acyl chains (e.g., Kariel et al., 1991; Hernandez-Borrell and Keough, 1993) as well as with ideas proposed by Litman and Mitchell regarding the manner in which cholesterol may interact with PCs that contain saturated sn-1 chains and highly unsaturated sn-2 chains (Litman and Mitchell, 1996). In the postulated PC packing model, the saturated sn-1 chains of the phospholipids pack in domains so that sn-1 chain interactions tend to maximize, whereas sn-2 chains tend to form the interface between

domains and determine the lateral packing properties of the system. Because cholesterol would interact preferentially with saturated sn-1 acyl chains, the sterol would tend to localize in the interior of the domains. However, the domain interfaces would still be formed by sn-2 chains and the lateral packing properties would still be determined primarily by the sn-2 chain properties. The steroid-hydrocarbon contacts need not be of a static, long-lived nature, i.e., complexation, but could be a time-averaged, dynamic effect. Interestingly, recent molecular dynamics computer simulations indicate that cholesterol produces a larger fraction of trans dihedral torsions in the upper half of the sn-1 chain than in the same region of the sn-2 chain of di-14:0 PC (Robinson et al., 1995).

The data obtained here clearly illustrate the major effect that PC acyl structure has on the elastic packing interactions that occur upon mixing with cholesterol. Mammalian cells, by manipulating the levels of their cholesterol and fluid-phase PCs with acyl chains of various unsaturation levels, have the capacity to produce localized regions within membranes that differ considerably in their in-plane elasticity. Such localized regions are likely to be very important in regulating a variety of processes including protein insertion, sorting, and activity.
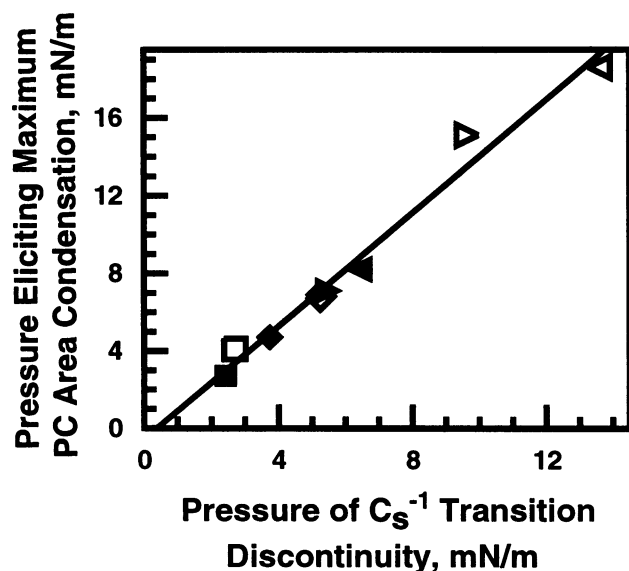
FIGURE 12 Correlation between surface pressure eliciting maximum PC area condensation and surface pressure at C_s^{-1} transition discontinuity. PC molecular species, mixed with equimolar cholesterol, are indicated by the following symbols: 16:0–18:1 PC = (■); 16:0–18:2 PC = (♦); 16:0–20:4 PC = (▶); 16:0–22:6 PC = (◀); di-18:1 PC = (□); di-18:2 PC = (◇); di-20:4 PC = (▷); di-22:6 PC = (◁). The surface pressure corresponding to the major discontinuity in C_s^{-1} for each PC species (mixed with equimolar cholesterol) was obtained from Figs. 3 through 10. The surface pressure eliciting maximum area condensation of each PC species (mixed with equimolar cholesterol) was obtained from Fig. 11.

REFERENCES

Albrecht, O., H. Gruler, and E. Sackmann. 1981. Pressure-composition phase diagrams of cholesterol/lecithin, cholesterol/phosphatidic acid, and lecithin/phosphatidic acid mixed monolayers: a Langmuir film balance study. J. Colloid Interface Sci. 79:319–338.

Ali, S., J. M. Smaby, H. L. Brockman, and R. E. Brown. 1994. Cholesterol's interfacial interactions with galactosylceramides. Biochemistry. 33:2900–2906.

Bartlett, G. R. 1959. Phosphorus assay in column chromatography. J. Biol. Chem. 234:466–468.

Behroozi, F. 1996. Theory of elasticity in two dimensions and its application to Langmuir-Blodgett films. Langmuir. 12:2289–2291.

Blume, A. 1979. A comparative study of the phase transitions of phospholipid bilayers and monolayers. Biochim. Biophys. Acta. 557:32–44.

Cadenhead, D. A., and F. Müller-Landau. 1980. Molecular accommodation and molecular interactions in mixed insoluble monomolecular films. J. Colloid Interface Sci. 78:269–270.

Chapman, D., N. F. Owens, M. C. Phillips, and D. A. Walker. 1969. Mixed monolayers of phospholipids and cholesterol. Biochim. Biophys. Acta. 183:458–465.

Davies, J. T., and E. K. Rideal. 1963. Interfacial Phenomena, 2nd. Ed. Academic Press, New York. 265.

Demel, R. A., W. S. M. Geurts van Kessel, and L. L. M. van Deenen. 1972. The properties of polyunsaturated lecithins in monolayers and liposomes and the interactions of these lecithins with cholesterol. Biochim. Biophys. Acta. 266:26–40.

The caption for the y-axis of the figure reads: "Pressure Eliciting Maximum PC Area Condensation, mN/m" and the x-axis reads: "Pressure of C_s^{-1} Transition Discontinuity, mN/m"

Demel, R. A., W. S. M. Geurts van Kessel, R. F. A. Zwaal, B. Roelofsen, and L. L. M. van Deenen. 1975. Relation between various phospholipase actions on human red cell membranes and the interfacial phospholipid pressure in monolayers. *Biochim. Biophys. Acta.* 406:97–107.

Evans, E., and D. Needham. 1987. Physical properties of surfactant bilayer membranes: thermal transitions, elasticity, rigidity, cohesion, and colloidal interactions. *J. Phys. Chem.* 91:4219–4228.

Evans, E., and W. Rawicz. 1990. Entropy driven tension and bending elasticity in condensed fluid membranes. *Phys. Rev. Lett.* 64: 2094–2097.

Evans, E. A., and R. Waugh. 1977. Mechano-chemistry of closed vesicular membrane systems. *J. Colloid Interface Sci.* 60:286–298.

Evans, R. W., M. A. Williams, and J. Tinoco. 1987. Surface areas of 1-palmitoyl phosphatidylcholines and their interactions with cholesterol. *Biochem. J.* 245:455–462.

Feng, S.-S., H. L. Brockman, and R. C. MacDonald. 1994. On osmotic-type equations of state for liquid-expanded monolayers of lipids at the air-water interface. *Langmuir.* 10:3188–3194.

Feng, S.-S., and R. C. MacDonald. 1995. Effects of chain unsaturation on the equation of state for lipid monolayers at the air-water interface. *Biophys. J.* 69:460–469.

Ghosh, D., M. A. Williams, and J. Tinoco. 1973. The influence of lecithin structure on their monolayer behavior and interactions with cholesterol. *Biochim. Biophys. Acta.* 291:351–362.

Hernandez-Borrell, J., and K. M. W. Keough. 1993. Heteroacid phosphatidylcholines with different amounts of unsaturation respond differently to cholesterol. *Biochim. Biophys. Acta.* 1153:277–282.

Hirshfeld, C. L., and M. Seul. 1990. Critical mixing in monomolecular films: pressure-composition phase diagram of a two-dimensional binary mixture. *J. Physiol. (Paris).* 51:1537–1552.

Holte, L. L., S. A. Peter, T. M. Sinnwell, and K. Gawrisch. 1995. ^{2}H nuclear magnetic resonance order parameter profiles suggest a change of molecular shape for phosphatidylcholines containing a polyunsaturated acyl chain. *Biophys. J.* 68:2396–2403.

Holte, L. L., F. Separovic, and K. Gawrisch. 1996. Nuclear magnetic resonance investigation of hydrocarbon chain packing in bilayers of polyunsaturated phospholipids. *Lipids.* 31:S-199–S-203.

Hui, S.-W., M. Cowden, D. Papahadjopoulos, and D. F. Parsons. 1975. Electron diffraction study of hydrated phospholipid single bilayers. Effects of temperature, hydration, and surface pressure of the "precursor" monolayer. *Biochim. Biophys. Acta.* 382:265–275.

Kariel, N., E. Davidson, and K. M. W. Keough. 1991. Cholesterol does not remove the gel-liquid crystalline phase transition of phosphatidylcholines containing two polyenoic acyl chains. *Biochim. Biophys. Acta.* 1062:70–76.

Keough, K. M. W., B. Giffin, and P. L. J. Matthews. 1989. Phosphatidylcholine-cholesterol interactions: bilayers of heteroacid lipids containing linoleate lose calorimetric transitions at low cholesterol concentration. *Biochim. Biophys. Acta.* 983:51–55.

Kuwae, T., P. C. Schmid, and H. H. O. Schmid. 1997. Alterations of fatty acyl turnover in macrophage glycerolipids induced by stimulation. Evidence for enhanced recycling of arachidonic acid. *Biochim. Biophys. Acta.* 1344:74–86.

Kwok, R., and E. Evans. 1981. Thermoelasticity of large lecithin bilayer vesicles. *Biophys. J.* 35:637–652.

Litman, B. J., and D. C. Mitchell. 1996. A role for phospholipid polyunsaturation in modulating membrane protein function. *Lipids.* 31:S-193–S-197.

Lund-Katz, S., H. M. Laboda, L. R. McLean, and M. C. Phillips. 1988. Influence of molecular packing and phospholipid type on rates of cholesterol exchange. *Biochemistry.* 27:3416–3423.

MacDonald, R. C., and S. A. Simon. 1987. Lipid monolayer states and their relationships to bilayers. *Proc. Natl. Acad. Sci. USA.* 84:4089–4093.

Marsh, D. 1996. Lateral pressure in membranes. *Biochim. Biophys. Acta.* 1286:183–223.

McConnell, H. M. 1996. Equilibration rates in lipid monolayers. *Proc. Natl. Acad. Sci. USA.* 93:15001–15003.

McConnell, H. M., and R. D. Koker. 1996. Equilibrium thermodynamics of lipid monolayer domains. *Langmuir.* 12:4897–4904.

Middleton, S. R., and B. A. Pethica. 1981. Electric field effects on monolayers at the air-water interface. *Faraday Symp. Chem. Soc.* 16:109–123.

Mitchell, D. C., M. Straume, and B. J. Litman. 1992. Role of sn-1-saturated, sn-2-polyunsaturated phospholipids in control of membrane receptor conformational equilibrium: effects of cholesterol and acyl chain unsaturation on the metarhodopsin I-metarhodopsin II equilibrium. *Biochemistry.* 31:662–670.

Needham, D. 1995. Cohesion and permeability of lipid bilayer vesicles. *In* Permeability and Stability of Lipid Bilayers. E. A. Disalvo and S. A. Simon, editors. CRC Press, Boca Raton, FL. 49–76.

Needham, D., T. J. McIntosh, and E. Evans. 1988. Thermomechanical and transition properties of dimyristoylphosphatidylcholine/cholesterol bilayers. *Biochemistry.* 27:4668–4673.

Needham, D., and R. S. Nunn. 1990. Elastic deformation and failure of lipid bilayer membranes containing cholesterol. *Biophys. J.* 58: 997–1009.

Osborn, T. D., and P. Yager. 1995. Modeling success and failure of Langmuir-Blodgett transfer of phospholipid bilayers to silicon dioxide. *Biophys. J.* 68:1364–1373.

Parks, J. S., and T. Y. Thuren. 1993. Decreased binding of apoA-1 to phosphatidylcholine monolayers containing 22:6 n-3 in the sn-2 position. *J. Lipid Res.* 34:779–788.

Pethica, B. A. 1955. The thermodynamics of monolayer penetration at constant area. *Faraday Trans. Soc.* 51:1402–1411.

Phillips, M. C. 1972. The physical state of phospholipids and cholesterol in monolayers, bilayers, and membranes. *Prog. Surf. Membr. Sci.* 5:139–221.

Phillips, M. C., and D. Chapman. 1968. Monolayer characteristics of saturated 1,2-diacyl phosphatidylcholines (lecithins) and phosphatidylethanolamines at the air-water interface. *Biochim. Biophys. Acta.* 163:301–313.

Robinson, A. J., W. G. Richards, P. J. Thomas, and M. M. Hann. 1995. Behavior of cholesterol and its effect on head group and chain conformations in lipid bilayers: a molecular dynamics study. *Biophys. J.* 68:164–170.

Schwarz, G., G. Wackerbauer, and S. E. Taylor. 1996. Partitioning of a nearly insoluble lipid monolayer into its aqueous subphase. *Colloids Surf.* 111:39–47.

Smaby, J. M., and H. L. Brockman. 1990. Surface dipole moments of lipids at the argon-water interface. Similarities among glycerol-ester-based lipids. *Biophys. J.* 58:195–204.

Smaby, J. M., and H. L. Brockman. 1991a. A simple method for estimating surfactant impurities in solvents and subphases used for monolayer studies. *Chem. Phys. Lipids.* 58:249–252.

Smaby, J. M., and H. L. Brockman. 1991b. Evaluation of models for surface pressure-area behavior of liquid-expanded monolayers. *Langmuir.* 7:1031–1034.

Smaby, J. M., and H. L. Brockman. 1992. Characterization of lipid miscibility in liquid-expanded monolayers at the gas-liquid interface. *Langmuir.* 8:563–570.

Smaby, J. M., H. L. Brockman, and R. E. Brown. 1994. Cholesterol's interfacial interactions with sphingomyelins and phosphatidylcholines: hydrocarbon chain structure determines the magnitude of condensation. *Biochemistry.* 33:9135–9142.

Smaby, J. M., H. L. Brockman, and R. E. Brown. 1995. Interfacial compressibility changes induced by cholesterol's interactions with sphingomyelins and phosphatidylcholines. *Biophys. J.* 68:98a (Abstr.).

Smaby, J. M., H. L. Brockman, and R. E. Brown. 1997. in *Biochemistry.* 36:2338—errata for: Cholesterol's interfacial interactions with sphingomyelins and phosphatidylcholines: hydrocarbon chain structure determines the magnitude of condensation. 1994. *Biochemistry.* 33: 9135–9142.

Smaby, J. M., V. S. Kulkarni, M. Momsen, and R. E. Brown. 1996a. The interfacial elastic packing interactions of galactosylceramides, sphingomyelins, and phosphatidylcholines. *Biophys. J.* 70:868–877.

Smaby, J. M., M. Momsen, V. S. Kulkarni, and R. E. Brown. 1996b. Cholesterol-induced interfacial area condensations of galactosylceramides and sphingomyelins with identical acyl chains. *Biochemistry.* 35: 5696–5704.

Steponkus, P. L., M. Uemura, and M. S. Webb. 1995. Freeze-induced destabilization of cellular membranes and lipid bilayers. *In* Permeability and Stability of Lipid Bilayers. E. A. Disalvo and S. A. Simon, editors. CRC Press, Boca Raton, FL. 77–104.

Stillwell, W., T. Dallman, A. C. Dumaual, F. T. Crump, and L. J. Jenski. 1996. Cholesterol versus α-tocopherol: effects on properties of bilayers made from heteroacid phosphatidylcholines. *Biochemistry*. 35: 13353–13362.

Subramaniam, S., and H. M. McConnell. 1987. Critical mixing in monolayer mixtures of phospholipid and cholesterol. *J. Phys. Chem.* 91: 1715–1718.

Vanderkooi, G. 1994. Computation of mixed phosphatidylcholine-cholesterol bilayer structures by energy minimization. *Biophys. J.* 66: 1457–1468.

Wolfe, D. H., and H. L. Brockman. 1988. Regulation of the surface pressure of lipid monolayers and bilayers by the activity of water: derivation and application of an equation of state. *Proc. Natl. Acad. Sci. USA*. 85:4285–4289.

Zerouga, M., L. J. Jenski, and W. Stillwell. 1995. Comparison of phosphatidylcholines containing one or two docosahexenoic acyl chains on properties of phospholipid monolayers and bilayers. *Biochim. Biophys. Acta*. 1236:266–272.